

## **A Possible Anticancer Drug Delivery System Based on Carbon Nanotube-Dendrimer Hybrid Nanomaterials**

**Ebrahim Mehdipoor<sup>a</sup>, Mohsen Adeli\*<sup>a</sup>, Masoumeh Bavadi<sup>a</sup>, Pezhman Sasanpour<sup>b</sup>, Bizhan Rashidian<sup>c</sup>, Mahdieh Kalantari<sup>a</sup>**

<sup>a</sup> *Department of Chemistry, Faculty of Science, Lorestan University, Khoramabad, Iran. Fax: (+98)661-2202782; Tel: (+98)916-3603772; E-mail: mohadeli@yahoo.com*

<sup>b</sup> *Institute for Nanoscience and Technology, Sharif University of Technology, Tehran, Iran*

<sup>c</sup> *Department of Electrical Engineering, Sharif University of Technology, Tehran, Iran*

### **Experimental**

#### *Materials*

MWCNT were prepared by chemical vapor deposition procedure in the presence of Co/Mo/MgO as catalyst at 900 °C. Citric acid monohydrate (MW=210.14), poly ethylene glycol (MW=1000), CDDP, [Fe (NO<sub>3</sub>)<sub>3</sub>.9H<sub>2</sub>O] and HNO<sub>3</sub> were purchased from Merck. The cell lines (mouse tissue connective fibroblast adhesive cells (L929) were obtained from the National Cell Bank of Iran (NCBI) Pasteur institute, Tehran, Iran. MTT powder, Annexin-V FLUOS Staining Kit, was obtained from Sigma.

#### *Characterization*

Nuclear magnetic resonance (<sup>1</sup>H NMR) spectra were recorded in D<sub>2</sub>O solution on a Bruker DRX 400 (400 MHz) apparatus with the solvent proton signal for reference. Infrared spectroscopy (IR) measurements were performed using a Nicolet 320 FT-IR. Ultraviolet (UV) spectra were recorded on a shimadzu (1650 PC) scanning spectrophotometer. Ultrasonic bath (Model: 5RS, 22 KHZ, Made in Italy) was used to disperse materials in solvents. The particle size, polydispersity and zeta potential of materials were determined using Dynamic Light Scattering (DLS) (zetasizer ZS, Malvern Instruments).

Morphology and size of materials were investigated using the Philips XL30 scanning electron microscope (SEM) with 12 and 15 A accelerating voltages.

Surface imaging studies were performed using atomic force microscopy (AFM) to estimate surface morphology and particle size distribution. The samples were imaged with the aid of Dualscope/Rasterscope C26, DME, Denmark, using DS 95-50-E scanner with vertical z-axis resolution of 0.1 nm. Raman spectra was obtained with an Almega Thermo Nicolet Dispersive Raman Spectrometer with second harmonic @532 nm of a Nd:YLF laser.

Thermogravimetric analysis (TGA) was performed on a PL-STA 1500 thermal analyzer set up under dynamic atmosphere of an inert gas (i.e. Ar) at 10 ml/min (room temperature). The Transmission electron microscopic (TEM) analyses were performed by a LEO 912AB electron microscope with accelerating voltage of 200 kV. The X-ray power diffraction pattern of products were recorded on Siemens D-500 diffractometer with Cu K $\alpha$  radiation ( $\lambda = 1.54056 \text{ \AA}$ ) in  $2\theta$  range from  $15^\circ$  to  $80^\circ$ .

The magnetic moment (M) of the hybrid nanomaterials was measured using Lake Shore model 7400 Vibrating Sample Magnetometer (VSM).

Simulation for NDDSs in the magnetic field was performed using Finite element method COMSOL multiphysics software.

#### *Preparation of CNT/ $\gamma$ -Fe<sub>2</sub>O<sub>3</sub>NP hybrid materials*

CNT/ $\gamma$ -Fe<sub>2</sub>O<sub>3</sub>NP hybrid materials were prepared according to reported procedures in literature [1].

#### *Preparation of PCA-PEG-PCA copolymers*

PCA-PEG-PCA copolymers were prepared according to reported procedures in literature [2].

#### *Preparation of CDDP-PCA-PEG-PCA-CDDP prodrugs*

CDDP (0.33mmol) was suspended in 10 ml distilled water and mixed with silver nitrate ([AgNO<sub>3</sub>]/ [CDDP] =1) to form the aqueous complex. The solution was kept in dark at room temperature to appear AgCl precipitate. Then, the mixture was centrifuged at 7000 rpm for 20 min to remove the AgCl precipitates. Afterward, the supernatant was purified by passing through a 0.45 mm filter and PCA-PEG-PCA linear-dendritic copolymer (0.03 g) was added to above solution and gently stirred for 48 h at 37 °C to obtain the CDDP-PCA-PEG-PCA-CDDP conjugate [3]. Yield or reaction was 55%.

### *Preparation of PCA-PEG-PCA/CNT/ $\gamma$ -Fe<sub>2</sub>O<sub>3</sub>NP and CDDP/PCA-PEG-PCA/CNT/ $\gamma$ -Fe<sub>2</sub>O<sub>3</sub>NP hybrid nanomaterials*

Typically, Fe<sub>2</sub>O<sub>3</sub>NP (0.001 g) was dispersed in 5 ml water and mixture was added to a water solution of PCA-PEG-PCA linear-dendritic copolymer (0.0024 g in 5 ml) (or CDDP-PCA-PEG-PCA-CDDP prodrug 0.00025 g in 5 ml) dropwise at room temperature and upon vigorous stirring. Then mixture was sonicated for 30 min at room temperature and it was filtrated to obtain a clear brown solution. Yield of reactions for preparation of PCA-PEG-PCA/CNT/ $\gamma$ -Fe<sub>2</sub>O<sub>3</sub>NP and CDDP/PCA-PEG-PCA/CNT/ $\gamma$ -Fe<sub>2</sub>O<sub>3</sub>NP hybrid nanomaterials was 50% and 65% respectively.

### *Cell culture*

Mouse tissue connective fibroblast adhesive cells (L929) were cultivated in RPMI-1640 medium supplemented with 10% fetal bovine serum, 2mM L-glutamine, 100 U/ml of penicillin, and 100  $\mu$ g/ml of streptomycin sulfate at 37°C in a humidified incubator with 5% CO<sub>2</sub>. The cells were maintained in an exponential growth phase by periodic subcultivation.

### *Cytotoxicity assay*

In vitro cytotoxicity of the nanomaterials was determined by 3-(4, 5-dimethylthiazol-2-yl)-2, 5-diphenyltetrazolium bromide (MTT) assay. The cells (2500 cells/well) were seeded in 96-well plates. Nanomaterials (5 and 1000  $\mu$ g/ml) were then added to the wells in triplicates and incubated for 72 hours. After the incubation period, 20  $\mu$ l of MTT dye (5 mg/ml in PBS) was added to each well, and they were incubated in the dark at 37 °C for 5 hours. Then media were removed and formazan crystals were dissolved in 200  $\mu$ L dimethylsulfoxide (DMSO) and 20  $\mu$ l of glycine buffer. Then the absorbance of each well was measured by an ELISA reader (Statfax–2100 Awareness Technology, USA) at 570 nm.

Cell viability was calculated using the following equation:

$$\text{Cell viability (\%)} = (\text{Ints}/\text{Intscontrol}) \times 100$$

Where “Ints” is the colorimetric intensity of the cells incubated with the samples, and “Intscontrol” is the colorimetric intensity of the cells incubated with the Media only (positive control).

### *Outlier Detection*

All MTT experiments were performed in triplicate or more, with the results expressed as mean  $\pm$  standard deviation; standard deviation values are indicated as error bars in the MTT results plots. The results were statistically processed for outlier detection using a “T procedure”<sup>(REF)</sup> using MINITAB software (Minitab Inc., State College, PA). One-way analysis of variance (ANOVA) with  $p < 0.05$  was performed for each set of MTT assay test repeats. Outlier samples have then been excluded from the corresponding asset viability calculations.

In this method, a  $T$ -ratio is calculated as follows

$$T = \frac{X - \bar{X}}{S}$$

Where  $X$  the suspected outlier is point (normally the smallest or the largest value in a set of measurements),  $\bar{X}$  is the sample mean, and  $S$  is the (estimated) standard deviation. If the calculated value of  $T$  is equal to or exceeds a critical value, the outlier point is removed with a significance level of 0.05. In the latter case, assuming that the data were sampled from a normal distribution, there is at least a 95% chance that the suspected point is in fact far from other points.

## Results and Discussion

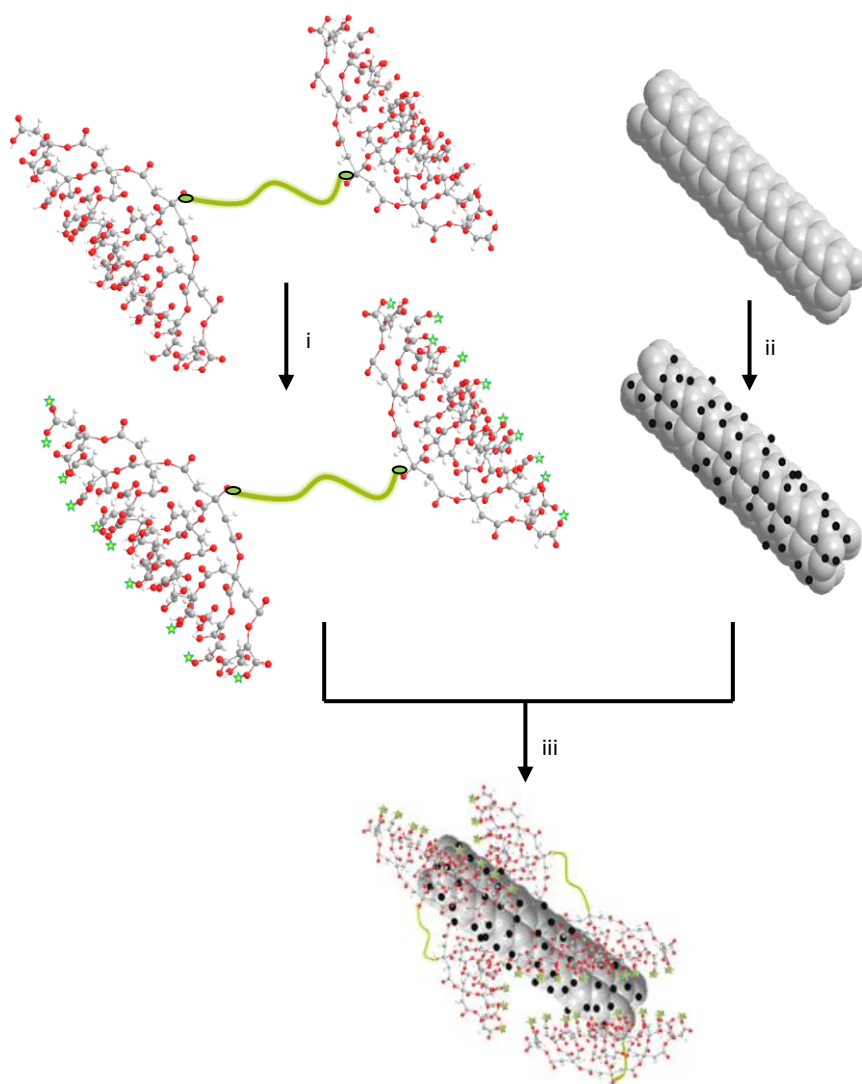


**Figure 1.** Synthetic route for preparation of hybrid nanomaterials, i) Water, 37 °C, cisplatin, ii) HNO<sub>3</sub>/H<sub>2</sub>SO<sub>4</sub> (3/1), 120 °C, 24 h, [Fe (NO<sub>3</sub>)<sub>3</sub>. 9H<sub>2</sub>O], iii) Water, 25°C, 30 min.

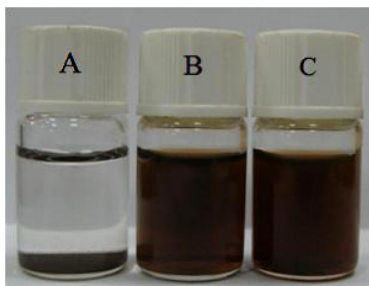


**Figure 2.** Hybrid nanomaterials suspensions in water after three months, (a) CNT/ $\gamma$ -Fe<sub>2</sub>O<sub>3</sub>NP, (b) PCA-PEG-PCA/CNT/ $\gamma$ -Fe<sub>2</sub>O<sub>3</sub>NP, (c) CDDP/PCA-PEG-PCA/CNT/ $\gamma$ -Fe<sub>2</sub>O<sub>3</sub>NP hybrid nanomaterials.

IR spectra were used to prove the synthesis of hybrid nanomaterials and evaluate interactions between their species. Figure (3a-g) shows the IR spectra of CDDP, Opened MWCNTs, CNT/ $\gamma$ -Fe<sub>2</sub>O<sub>3</sub>NP, PCA-PEG-PCA, CDDP/PCA-PEG-PCA, PCA-PEG-PCA/CNT/ $\gamma$ -Fe<sub>2</sub>O<sub>3</sub>NP and CDDP/PCA-PEG-PCA/CNT/ $\gamma$ -Fe<sub>2</sub>O<sub>3</sub>NP hybrid nanomaterials.

In the IR spectrum of CDDP (figure 3a), absorbance peak at 3415–3205 cm<sup>-1</sup> can be assigned to amino functional groups, and the absorbance peaks at 1622 and 1541 cm<sup>-1</sup> correspond to the stretching vibrations of –N-H group. The IR spectrum of the Opened MWCNTs showed an absorbance band at 1700 cm<sup>-1</sup> assigned to the carbonyl groups created on the surface and tips of carbon nanotubes, in agreement with the reported results in literature [4]. Furthermore, sharp absorbance peaks are observed at low frequency region (532 and 449 cm<sup>-1</sup>) in the IR spectrum of CNT/ $\gamma$ -Fe<sub>2</sub>O<sub>3</sub>NP, which could be ascribed to the Fe–O bond vibrations in the  $\gamma$ -Fe<sub>2</sub>O<sub>3</sub> nanoparticles.

From the PCA-PEG-PCA spectrum (figure 3d), distinctive absorption peaks appeared at 1735 and 1645 cm<sup>-1</sup> (acidic carbonyl and esteric groups respectively) and 1101 cm<sup>-1</sup> (skeletal vibration involving the C–O stretching). The broad absorption peak at 3600–3000 cm<sup>-1</sup> was assigned to stretching vibration of hydroxyl groups.

The IR spectrum of CDDP/PCA-PEG-PCA showed obvious alterations in comparison with the IR spectrum of PCA-PEG-PCA, indicating the conjugation of the CDDP molecules to PCA-PEG-PCA linear-dendritic copolymer surfaces via carboxylate groups. For example, absorbance

band of carbonyl functional groups is shifted towards lower frequencies (around  $18\text{ cm}^{-1}$ ) showing that these functional groups are coordinated to platinum of CDDP. On the other hand due to the overlapping of absorbance band of amino functional groups of CDDP a shift toward higher frequencies can be seen for absorbance band of hydroxyl functional groups.

By comparison figures 3c, d with 3f, it can be found that characteristic peaks of PCA-PEG-PCA and CNT/ $\gamma$ - $\text{Fe}_2\text{O}_3$ NP are appeared in the IR spectra of PCA-PEG-PCA/CNT/ $\gamma$ - $\text{Fe}_2\text{O}_3$ NP proving the preparation of this hybrid nanomaterials and non-covalent interactions between CNT/ $\gamma$ - $\text{Fe}_2\text{O}_3$ NP and PCA-PEG-PCA. In the IR spectrum of PCA-PEG-PCA/CNT/ $\gamma$ - $\text{Fe}_2\text{O}_3$ NP absorbance peaks at  $532$  and  $449\text{cm}^{-1}$  assigned to the  $\tilde{\alpha}$ - $\text{Fe}_2\text{O}_3$  nanoparticles of CNT/ $\gamma$ - $\text{Fe}_2\text{O}_3$ NP are shifted to the  $526$  and  $457\text{cm}^{-1}$  and absorbance peak at  $1645\text{ cm}^{-1}$  ascribed to the esteric groups of PCA-PEG-PCA are shifted to the  $1616\text{ cm}^{-1}$ . All these changes indicate the interfacial interaction between CNT/ $\gamma$ - $\text{Fe}_2\text{O}_3$ NP and PCA-PEG-PCA and clearly indicate that the functional moieties of PCA-PEG-PCA are attached to the surface of the CNT/ $\gamma$ - $\text{Fe}_2\text{O}_3$ NP.

Evidently, better evidence to prove interactions between all species of HNMDSSs can be found through comparison the IR spectrum of CDDP/PCA-PEG-PCA/CNT/ $\gamma$ - $\text{Fe}_2\text{O}_3$ NP hybrid nanomaterials with its precursors. The spectrum of CDDP/PCA-PEG-PCA/CNT/ $\gamma$ - $\text{Fe}_2\text{O}_3$ NP hybrid nanomaterials (figure 3g) and PCA-PEG-PCA/CNT/ $\gamma$ - $\text{Fe}_2\text{O}_3$ NP are of similar, outstandingly. Only, a shift in the absorbance band of ( $-\text{COO}-$ ) groups of linear-dendritic copolymer from  $1645$  to  $1596\text{ cm}^{-1}$  and appearance of new doublet bands around  $3380\text{ cm}^{-1}$ , assigned to the stretching of the N-H groups of cisplatin of CDDP/PCA-PEG-PCA/CNT/ $\gamma$ - $\text{Fe}_2\text{O}_3$ NP hybrid nanomaterials, show the conjugation of the CDDP to linear-dendritic copolymer through reaction of oxygen (as a strong base) of the carboxylate ( $-\text{COO}-$ ) ion with platinum (as a weak Lewis acid).

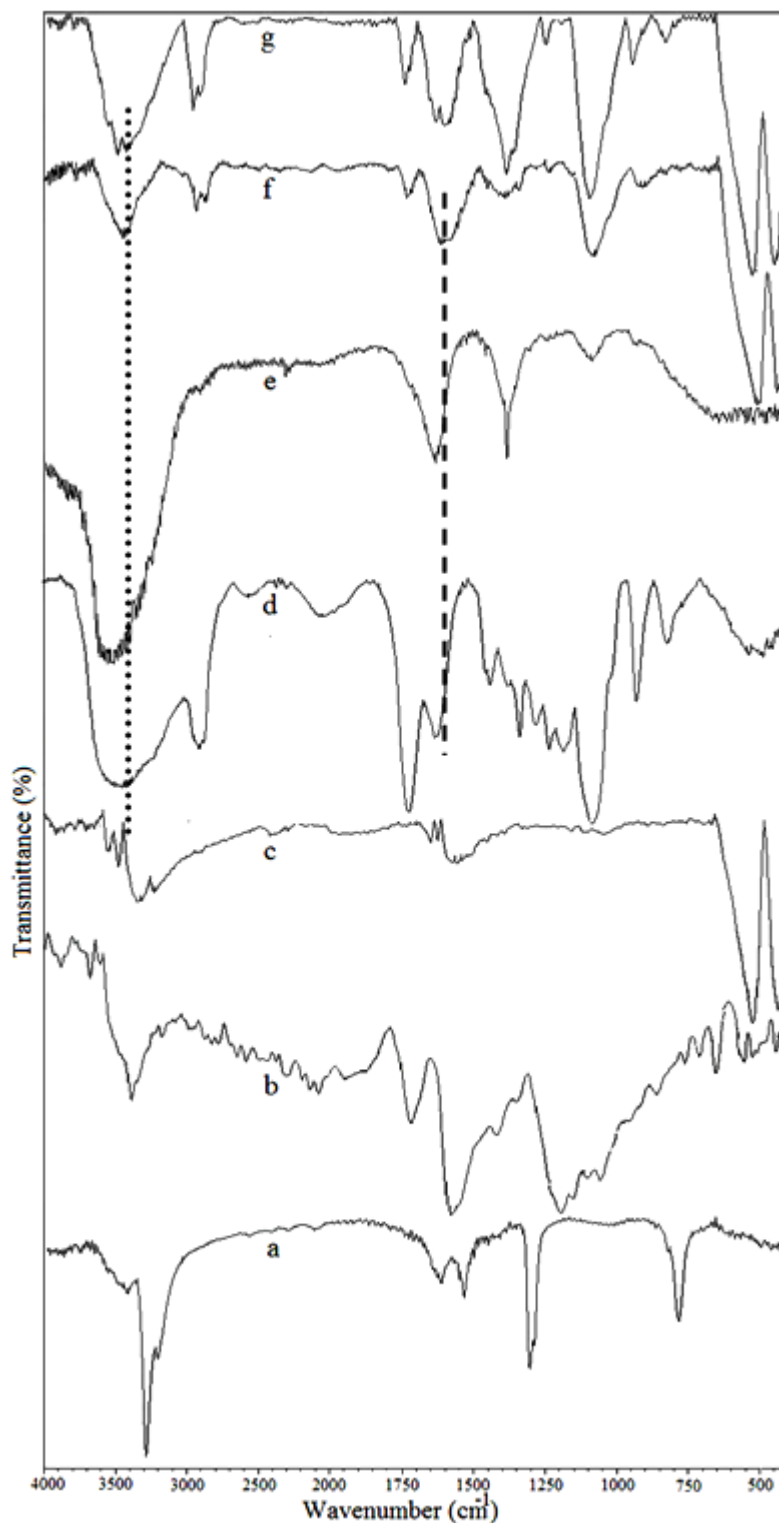


**Figure 3.** IR spectra of (a) CDDP (b) Opened CNTs, (c) CNT/ $\gamma$ -Fe<sub>2</sub>O<sub>3</sub>NP, (d) PCA-PEG-PCA, (e) CDDP/PCA-PEG-PCA, (f) PCA-PEG-PCA/CNT/ $\gamma$ -Fe<sub>2</sub>O<sub>3</sub>NP, (g) CDDP/PCA-PEG-PCA/CNT/ $\gamma$ -Fe<sub>2</sub>O<sub>3</sub>NP hybrid nanomaterials.



The TGA thermogram of CNT/ $\gamma$ -Fe<sub>2</sub>O<sub>3</sub>NP shows weight loss in three stages at 120, 274-332 and 400-600 °C which are attributed to the evaporation of physically adsorbed water (1%), loss of functional groups of  $\alpha$ -Fe<sub>2</sub>O<sub>3</sub> nanoparticles about 6% and the gradual decomposition of carbon nanotubes (7%) respectively. The weight loss of the PCA-PEG-PCA (TGA thermogram) occurs in two stages at 171-249 and 366-416°C which are attributed to decomposition of PCA blocks (51%) and the decomposition of the PEG block (43%), respectively.

Weight percent of PCA-PEG-PCA/Weight percent of conjugated drug molecules = 45/7 = 6.4

Molecular weight of PCA-PEG-PCA/Molecular weight of conjugated drug molecules = 3700/229 = 16

16/6.4= 2.5

Figure 4 shows the XRD patterns of the Opened MWNTs and  $\alpha$ -Fe<sub>2</sub>O<sub>3</sub> decorated MWNTs. From Fig. 4a, shows the XRD pattern of the Opened MWNTs. It can be seen that the diffraction peaks at  $2\theta = 26.4^\circ, 42.58^\circ$  are assigned to (002), (101) planes of MWNTs. Fig. 4b is the XRD pattern of the decorated MWNTs. The diffraction angles at  $2\theta = 35.52^\circ, 43.22^\circ, 57.87^\circ$  can be assigned to (3 1 1), (4 0 0), (511) crystal planes of  $\alpha$ -Fe<sub>2</sub>O<sub>3</sub>, respectively. The characteristic peaks of MWNTs in the spectrum of  $\alpha$ -Fe<sub>2</sub>O<sub>3</sub> decorated MWNTs still exist, which indicates that the structure of MWNTs is not destroyed during experiment.

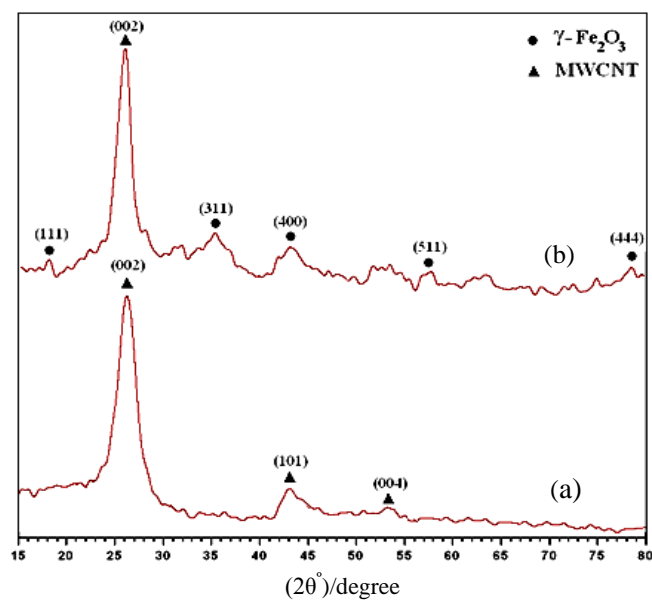


**Figure4.** XRD pattern of (a) opened MWCNTs, (b) CNT/ $\gamma$ -Fe<sub>2</sub>O<sub>3</sub>NP hybrid nanomaterials.

AFM images of PCA-PEG-PCA/CNT/ $\gamma$ -Fe<sub>2</sub>O<sub>3</sub>NP confirm that linear-dendritic copolymers are assembled onto the surface of CNTs. Non-continuous molecular self-assemblies of linear-dendritic copolymers onto the surface of CNTs axis show that interactions between linear-dendritic copolymers and CNTs surface change regionally (figures 5a and 5b). While hydrogen bonding between dendritic blocks of linear-dendritic copolymers and hydroxyl functional groups of iron oxide nanoparticles cause assembling of these copolymers onto the surface of CNT/ $\gamma$ -Fe<sub>2</sub>O<sub>3</sub>NP hybrid nanomaterials. Defects sites on sidewall of CNTs, where iron oxide nanoparticles are anchored, are more susceptible to attach molecular self-assemblies of linear-dendritic copolymers. Therefore non-continuous and lump-like assemblies around an axis in the AFM images are observed.

The same pattern was observed for AFM images of CDDP/PCA-PEG-PCA/CNT/ $\gamma$ -Fe<sub>2</sub>O<sub>3</sub>NP (figure 6a), but their phase contrast images show two phase for linear-dendritic copolymers proving that CDDP molecules are conjugated on their functional groups (figure 6b).

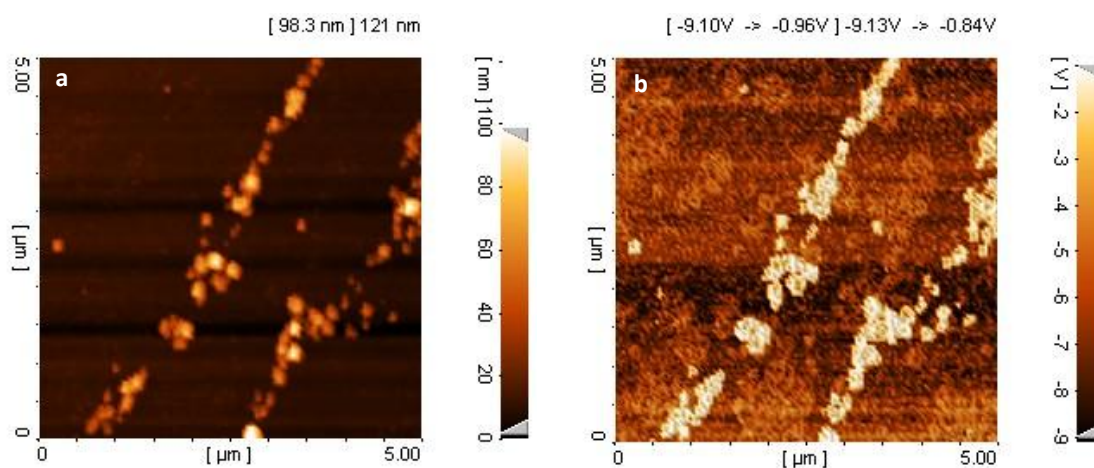


**Figure 5.** AFM images of PCA-PEG-PCA/CNT/ $\gamma$ -Fe<sub>2</sub>O<sub>3</sub>NP hybrid nanomaterials a) topographic and b) contrast phase images.

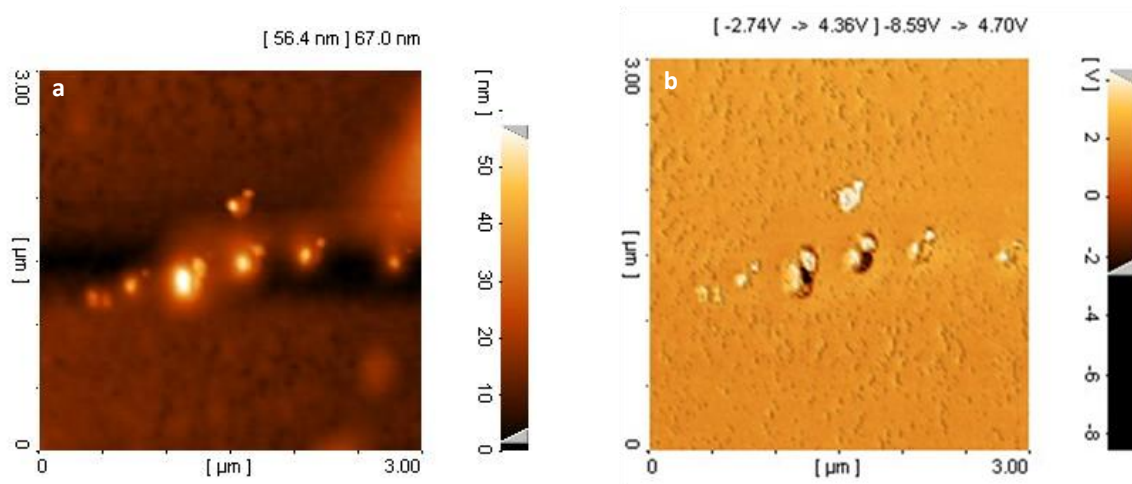


**Figure 6.** AFM images of CDDP/PCA-PEG-PCA/CNT/ $\gamma$ -Fe<sub>2</sub>O<sub>3</sub>NP hybrid nanomaterials a) topographic and b) contrast phase images.

While CNT/ $\gamma$ -Fe<sub>2</sub>O<sub>3</sub>NP hybrid nanomaterials are in their extended conformations and appear as long and thin strands with several micrometer lengths and 30 nm thickness in SEM images, PCA-PEG-PCA/CNT/ $\gamma$ -Fe<sub>2</sub>O<sub>3</sub>NP hybrid nanomaterials are quite different and they appear as short worm-like objects. Their length and thickness are around 500 and 50 nm respectively. Increasing the thickness of CNT/ $\gamma$ -Fe<sub>2</sub>O<sub>3</sub>NP is related to the self-assembling of linear-dendritic copolymers on their surface but decreased length is due to the changing of the conformation of CNTs from extended toward closed upon non-covalent interactions with linear-dendritic copolymers (Figure 7) [5].

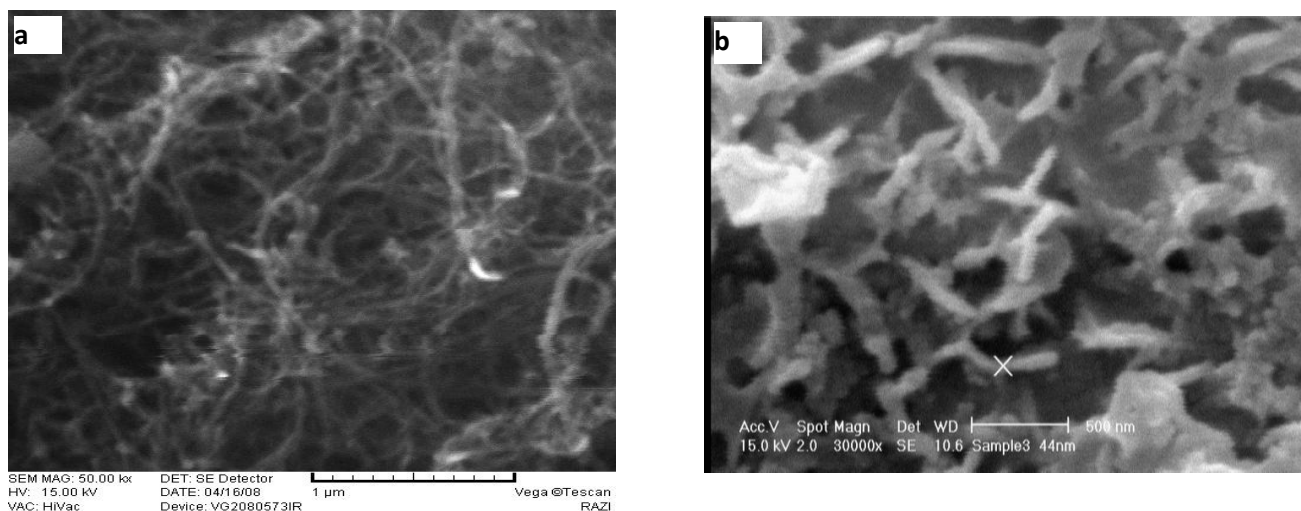


**Figure 7.** SEM images of (a) CNT/ $\gamma$ -Fe<sub>2</sub>O<sub>3</sub>NP, (b) PCA-PEG-PCA/CNT/ $\gamma$ -Fe<sub>2</sub>O<sub>3</sub>NP hybrid nanomaterials.

### Simulation for NDDSs in the magnetic field

As drug is localized with magnetic nanoparticles attached to it, one should use external magnetic field to position drug in desired location. In order to consider interaction of magnetic field with magnetic nanoparticles inside blood (ferrofluid), multiphysics modeling has been used. In the model, Maxwell's equation has been used for magnetic field and dynamic flow is governed with Navier Stokes equation [6]. Effect of magnetic field on the ferrofluid is applied inside Navier-Stokes through volume force field [7]. Systems of equations are solved using Finite element method with COMSOL Multiphysics software.

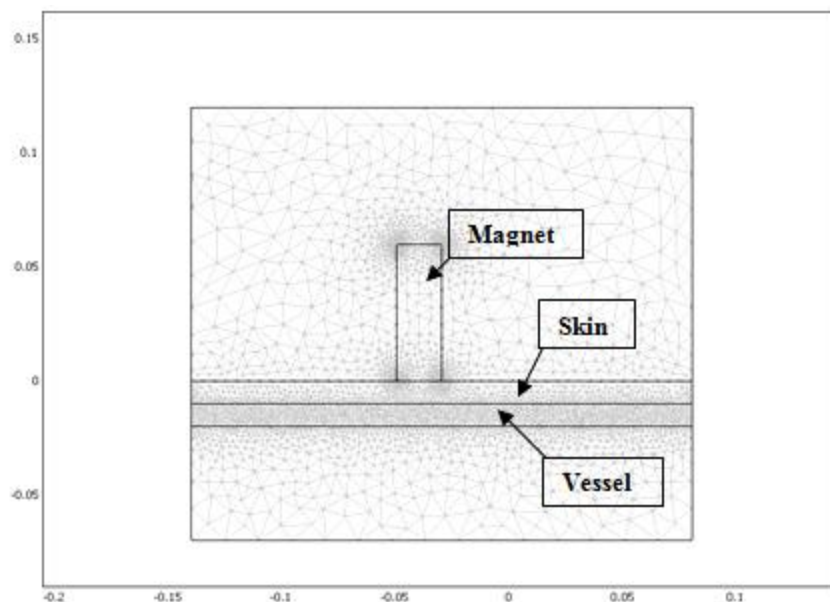


**Figure 8.** Geometry and Mesh Structure of Simulation Structure.

Figure 8 shows the geometry and mesh structure of numerical simulation. Structure consists of an external magnet which is used for magnetic field source. Two layers have been considered for vessel and skin structure. Ferrofluid is flowing in vessel structure. Boundary condition used for fluid injection inside the vessel is applied on left boundary of vessel and consists of sinusoidal pulse shape, describing heart beat.

Based on cytotoxicity results, CDDP/PCA-PEG-PCA/CNT/ $\gamma$ -Fe<sub>2</sub>O<sub>3</sub>NP hybrid nanomaterials entered the cells via endocytosis and drugs release after disassociation of hybrid nanomaterials

and cause cell death without accumulation in the cytoplasm respect to alone CNT/ $\gamma$ -Fe<sub>2</sub>O<sub>3</sub>NP (figure 9).



**Figure 9.** Mechanism of internalization the CDDP/PCA-PEG-PCA/CNT/ $\gamma$ -Fe<sub>2</sub>O<sub>3</sub>NP hybrid nanomaterials into the cancer cells.

## References

1. C. Huiqun, Z. Meifang, L. Yaogang, *Journal of Magnetism and Magnetic Materials* 2006, 305, 321.
2. A. Tavakoli Naeni, M. Adeli, M. Vossoughi, *Nanomedicine: Nanotechnology, Biology, and Medicine*, 2010, 6, 556.
3. H. Ye, L. Jin, R. Hu, Z. Yi, *Biomaterials* 2006, 27, 5958.
4. M. Adeli, N. Mirab, M. S. Alavidjeh, Z. Sobhani, F. Atyabi, *Polymer* 2009, 50, 3528.
5. M. Adeli, N. Mirab, F. Zabihi, *Nanotechnology*, 2009, 20, 485603(10pp).
6. M. A. Lohakan, *WSEAS Transactions on Mathematics* 2006, 5, 1309.
7. C. M. Oldenburg, S. E. Borglin, G. J. Moridis, *Transport in Porous Media* 2000, 38, 319.

